coatings

MDPI

Article

Transparent Superhydrophobic Coatings with Mechanical and Chemical Stability Prepared by Modified Polyhedral Oligosilsesquioxanes via UV-Curable Method

Weibiao Zhu [1,2], Yazhou Xu [1], Jinxin He [1,*] and Xia Dong [1]

[1] College of Chemistry and Chemical Engineering, Donghua University, Shanghai 201620, China
[2] Shanghai Hangyong Photoelectric New Material Co., Ltd., Shanghai 201600, China
* Correspondence: jxhe@dhu.edu.cn

Abstract: Superhydrophobic coating with applicable transmittance was synthesized by simple UV-curable method which was likely suitable for large-scale production. The super-hydrophobicity was derived from the component containing modified polyhedral oligomeric silsesquioxanes which was chosen for low free energy and the potential to form hierarchical structure. The coating adhesion could reach the highest level by strip tape peel test. Compared to the UV-cured commercial coatings, the coating adhesion is enhanced by at least two levels. Super-hydrophobicity was preserved after long duration of water droplet impact, while water contact angle decreased slightly after sand impact due to partial damage of hierarchical structure. The coating can resist chemical corrosion by acid solution (HCl), base solution (NaOH) and salt solution (NaCl). The coating with water repellence function, adequate transmittance, and good mechanical and chemical stability is of great interest for practical outdoor applications.

Keywords: coating; super-hydrophobicity; mechanical stability; chemical stability; polyhedral oligomeric silsesquioxanes component; polycarbonate

Citation: Zhu, W.; Xu, Y.; He, J.; Dong, X. Transparent Superhydrophobic Coatings with Mechanical and Chemical Stability Prepared by Modified Polyhedral Oligosilsesquioxanes via UV-Curable Method. *Coatings* **2023**, *13*, 498. https://doi.org/10.3390/coatings13030498

Academic Editor: Mohamed Selim

Received: 29 January 2023
Revised: 17 February 2023
Accepted: 22 February 2023
Published: 24 February 2023

1. Introduction

Super-hydrophobicity as unique surface wettability phenomenon means the contact angle of water droplets on the surface is greater than 150° and the sliding angle from the surface is less than 10° [1]. The interest in super-hydrophobicity research can be traced back to an early curiosity about the existence of superhydrophobic phenomena in nature [2–4]. For example, water droplets roll freely on the surface of lotus leaves [2], water striders walk and jump on the surface of water [3], dragonflies fly in rainy weather with their wings dry [4]. Inspired by these natural phenomena, the theoretical research and practical applications of superhydrophobic surface have been favored by a majority of researchers in decades. The reason for its rapid popularity is that the superhydrophobic material is valuable in a variety of areas in human daily life and industrial production, such as antifouling [5,6], anti-icing [7], anti-frosting [8], metal anti-corrosion [9], oil–water separation [10], waterproof fabric [11] and so on. With the development and prospect of various transparent optical products, such as automobile windshields, optical screens, architectural glass, solar photovoltaic panels and medical lenses [12–17], the demands of super-hydrophobicity, high transmittance, mechanical stability, chemical stability and large-scale production are urgent for applications in the mentioned fields. Super-hydrophobicity induced by an appropriate surface coating or a dedicated surface treatment seems to be effective [18]. However, the common preparation methods of superhydrophobic surfaces including template method [19], etching method [20], deposition method [21], sol-gel method [22], layer-by-layer self-assembly method [23], phase separation method [24] and electrospinning method [25] are apparently limited by complex processing process, high

equipment cost and narrow application range of substrate, resulting in difficulties in implementing large-scale production, processing and industrialization.

The construction of hierarchical structures by doping nanomaterials to enhance the super-hydrophobicity of the surface and to preserve original transmittance is an opportunity for large-scale application. Nevertheless, it is noteworthy that the structures which enhances the super-hydrophobicity may lead to mechanical and chemical frailty [26]. Polyhedral oligosilsesquioxanes or polyhedral oligomeric silsesquioxanes, abbreviated as POSS, is a kind of cage-like silsesquioxanes nanomaterials [27]. It has an inorganic silica core surrounded by an organic (preferably functional) group R that can be useful for polymerization or grafting reactions [28]. Due to low surface energy of POSS [29], coatings containing POSS could demonstrate superhydrophobic performance. In the construction process of superhydrophobic surface, there are two main difficulties: one is low transmittance, the other is the poor connection between coating and substrate. It is an urgent task for preparing transparent superhydrophobic coating with mechanical and chemical stability. In this work, in order to find solutions to the above problems, we put forward a simple construction scheme via UV-curing for superhydrophobic coating deposited on polycarbonate (PC) sheet. The technique is simple to operate and likely to be useable in large-scale production.

2. Materials and Methods

2.1. Materials

The material used as the substrate was polycarbonate (PC, 200 mm × 300 mm × 0.8 mm) purchased from Sichuan Longhua Photoelectric Film Co., Ltd. (Mianyang, Chian). Acrylate oligomer (product name 8110) was purchased from Allnex Resin (Suzhou, China) Co., Ltd. 2-methyl-4-methyl thio-2-morpholine phenylacetone (2-M-4-MT-2-MP, product name I-907, 98%) was purchased from Shanghai Aladdin Biochemical Technology Co., Ltd. (Shanghai, China). Anhydrous tetrahydrofuran (THF, 98%), anhydrous ethanol (ET, 99.5%), hydrochloric acid (HCl, 36.0%~38.0%), sodium hydroxide (NaOH, ≥96.0%) and sodium chloride (NaCl, ≥99.8%) were purchased from Sinopharm Chemical Reagents Co., Ltd. (Shanghai, China) 1.,6-Hexanediol diacrylate (HDDA) was purchased from Eternal Chemical Co., Ltd. (Kaohsiung, Taiwan). POSS (molecular weight 633.04, purity 98%) was purchased from Suzhou Xisuo Co., Ltd. (Suzhou, China). After modified via sulfhydrylation and fluorination, the POSS component was induced by mixing trivinyl sulfhydryl-penta-methylacrylate dodecyl fluoroheptyl-POSS (POSS-SH3-DFMA5) and vinyl-sulfhydryl-hepta-methylacrylate dodecyl fluoroheptyl-POSS (POSS-SH-DFMA7) synthesized in the laboratory at a ratio of 1:1.5. Water used in coating preparation and characterization was deionized.

2.2. Coating Preparation

The PC substrate was cut into a 30 mm × 30 mm square, and the protective films on both sides were gently torn off with tweezers. Ultrasonic cleaning was performed with ET and deionized water successively and dried in a clean environment.

According to the composition shown in Table 1, mixture suspension systems O and C1~C6 were obtained through mixing in an ultrasonic shock device for 20 min with 40% addition of ET.

Coated samples were prepared by spraying one of the mixture suspension systems (Table 1) onto the surface of PC substrate using 0.5 mm nozzle at 0.25 mL/s flow rate under 0.3 MPa compressed air pressure. The distance from PC substrate to nozzle was about 22~25 cm. In order to state briefly, the coatings were designated following the number of mixture suspension systems listed in Table 1.

Table 1. The composition of mixture suspension systems.

System NO.	Composition (wt. %)			
	Acrylate Oligomer(8110)	HDDA	POSS Component	2-M-4-MT-2-MP(I907)
O	64	32	-	4
C1	57	29	10	4
C2	51	25	20	4
C3	38	18	40	4
C4	31	15	50	4
C5	21	10	65	4
C6	14	7	75	4

Then, the coated samples were dried in an oven at 35 °C for 30 min and subsequent in a nitrogen atmosphere to expose to 10 mW/cm^2 UV curing at 365 nm for 1 min. During the coating preparation, acrylate oligomer(8110) is the key factor to form coatings, HDDA plays the role of connection between coating and substrate, and 2-M-4-MT-2-MP(I907) is used as UV initiator.

2.3. Characterization

The surface wettability of the coating was evaluated by water contact angle (WCA) and slip angle (SA) measured using a contact angle test system (DSA30, KRUSS, Hamburg, Germany). WCA and SA measurements were performed at five different locations for each sample, and the volume of the droplet was fixed at 5 μL. The transmittances of the coatings were measured with a UV-Visible Near-Infrared Spectrophotometer (UV-3600Plus, Shimadzu, Japan) in the wavelength range of 380~800 nm. Field emission scanning electron microscopy (SEM, SU8010, HITACHI, Tokyo, Japan) was used to characterize the micro structure morphology of coating.

3. Results and Discussion

3.1. Surface Wettability

The WCA and SA variations of PC substrate and the coatings are shown in Figure 1a. The WCA and SA values are listed in Table 2. From Figure 1a, the WCA variation of the coatings showed a trend of steady improvement with the linear increase of the addition of POSS component. Compared with the original PC substrate, WCA values of coatings O and C1~C6 are all increased. With the addition amount of POSS component increase, WCA values of the coatings increased implying the improved surface hydrophobicity. It can be seen that addition of POSS component plays an important role in the surface wettability. WCA values of coatings with addition of POSS component were more than 95° which meets the requirements of hydrophobic coating, while WCA value of PC substrate without addition of POSS component was less than 90°. The variation of SA was opposite from that of WCA following the addition amount of POSS component. It could be seen from Figure 1a and Table 2 that the hydrophobic character of the coating changed to a superhydrophobic character when the addition amount of POSS component was above 40% (coating C4~C6). For PC substrate, no matter how much angle tilted the surface, the droplets couldn't roll. However, with the increase of POSS component addition, the droplets on the surface changed from the original "bound" state to the present "free" state, SA value even decreased to 2°. Figure 1b showed the wetting state of water droplets deposited on the coating C5. The shape of droplets on the coating C5 looks like circle. In keeping with Figure 1c of the immersion state in water, the droplets could not wet the coating surface, indicating the super-hydrophobicity. The water used in Figure 1b,c is deionized. SEM image of the coating C5 in Figure 1d shows hierarchical morphology, another important factor for generating super-hydrophobicity.

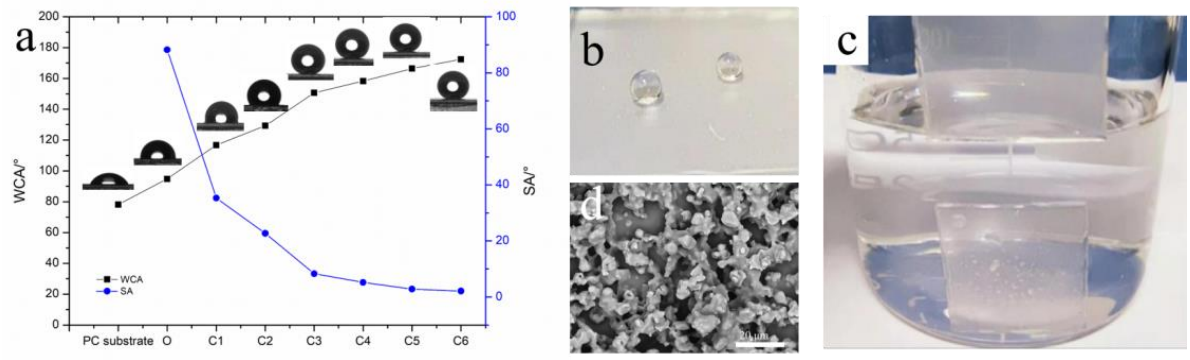

Figure 1. (**a**) WCA and SA variation of PC substrate, the coatings of O and C1~C6, here WCA is the abbreviation of Water Contact Angle and SA is the abbreviation of Slip Angle; (**b**) photograph of water droplets deposited on the coating surface of C5; (**c**) photograph of immersion state in water of the coating surface C5, (**d**) SEM image of the coating C5.

Table 2. WCA, SA and transmittance values of PC substrate and the coatings of O and C1~C6.

	PC Substrate	O	C1	C2	C3	C4	C5	C6
WCA (°)	78.2	94.8	116.7	129.3	150.6	158.2	166.4	172.4
SA (°)	-	88.2	35.3	22.7	8.3	5.2	2.8	2.1
Transmittance (%)	89.1	90.8	86.4	85.5	84.2	79.8	76.8	66.6

3.2. Transmittance

The transmittance listed in Table 2 referred to the average value in the wavelength range of 380~800 nm. The transmittance of PC substrate without coating was 89.1% (Table 2). The transmittances of PC with the coatings C1~C6 decreased with the increase of POSS component addition as illustrated in Figure 2. The coating C4 and C5 could achieve superhydrophobicity and the optical transmittance also met the requirement of use grade. In various fields of optical application, like outdoor optical display, not only the superhydrophobic property but also the visibility is vital. Although the coating C6 performs better super-hydrophobicity than the coating C4 and C5, its transmittance was lower, just 66.6%, which limits its practical application in transparent optics field. Integrated into account, coating C5 has more potential for use.

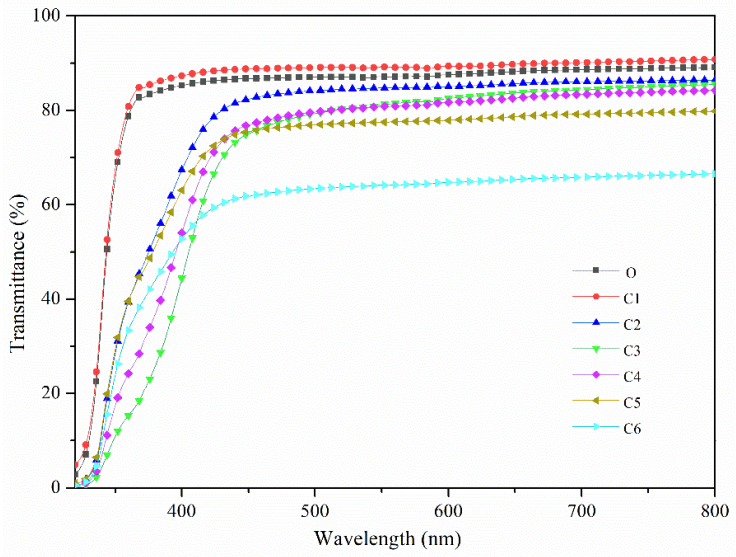

Figure 2. Transmittance spectra of the coatings O and C1~C6.

3.3. Mechanical Stability

As is well known, except for the function factors as super-hydrophobicity and transmittance, ability to bear mechanical wear is essential. According to the method described in ASTM D3359, strip tape peel test was used to test the coating adhesion. Water droplet impact test and sand impact test was used to evaluate the super-hydrophobicity retention ability of the coating, the WCA and SA values of the coating after a certain number of mechanical wear cycles were measured and recorded. The coating C5 was chosen to simulate the three frictional conditions in the practical application process (strip tape peel test, water droplet impact test and sand impact test).

3.3.1. Strip Tape Peel Test

In the strip tape peel test, 100 grids (1 mm × 1 mm) were scratched on the surface of coating C5 using a specially-made knife, and then a tape peeling test was performed on the coating surface with a tape (trade name of 3M 610) of 47 N/100 mm bonding strength. The coating surface images before and after tape stripping are shown in Figure 3a,b respectively. It could be observed that the scratching part of the superhydrophobic coating C5 was seldom affected by tape stripping. On the basis of described rating criteria [30], the adhesion rating of coating C5 was the highest level of coating adhesion (0 grade). The adhesion grade of traditional commercial hydrophobic coatings formed on PC by UV cured method generally lies in 2~3 grade range. [31] The coating adhesion of C5 is improved by at least 2 levels, compared to the commercial coatings.

3.3.2. Water Droplet Impact Test

For water droplet impact test, water droplets of about 22 μL each were released drop by drop to impact the surface of coating C5 at a rate of 1 drop/s through a constant pressure funnel at a height of 30 cm above the coating. WCA and SA values of the surface were recorded every 15 min. The results are shown in Figure 3c. After 3 h of water droplet impact (1.08×10^4 drops), the super-hydrophobicity of the coating disappeared. WCA decreased to 148.2°, and SA also increased observably, reaching to 12.7°. It was noteworthy that WCA of coating C5 undergoing water droplet impact returned to 161.0° after drying. The reason may be that when droplets impact the coating, the surface humidity gradually increases which is beneficial for wetting and leads to WCA decrease. The impact of 1.08×10^4 water droplets leads to partial damage of the protruding structure and even partial shedding of the coating surface as revealed in Figure 3d. Therefore, after drying, the WCA still saw a little decrease.

3.3.3. Sand Impact Test

Sand impact test was carried out by releasing sand particles at a height of 30 cm above the coating. The average diameter of sand particles was about 400 μm. The release rate of sand particles was controlled at 40 g/min. WCA and SA at different times were recorded in Figure 3e to reflect the superhydrophobic retention ability of the surface coating. When the sand impacted the surface of coating C5 for 12 min (about 480 g), although the coating was still hydrophobic, its superhydrophobic characteristics disappeared as its WCA decreased to 147.5° and SA increased to 16.4°. As can be seen from Figure 3f, compared with the coating surface impacted by water droplets, the hierarchical pattern of the coating surface impacted by sand particles was more seriously damaged. The area of hierarchical structures had been greatly reduced, leaving many flat "ruins". The microstructure damage of the coating surface was the main reasons for the failure of super-hydrophobicity. As the test simulates extreme harsh impact and the coating retains its hydrophobicity, the coating can resist sand impact to some degree.

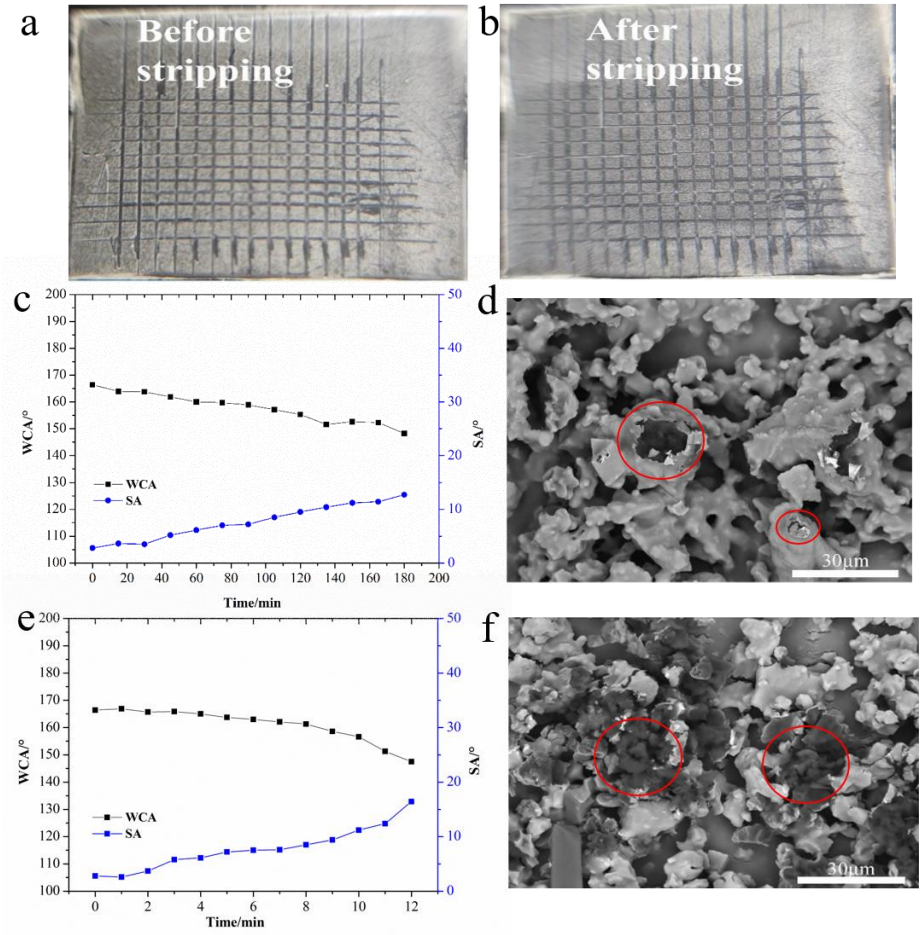

Figure 3. (**a**) Image before stripping; (**b**) image after stripping; (**c**) the change of WCA and SA during 3 h water droplet impact test; (**d**) SEM image of the coating after water droplets impact test; (**e**) the change of WCA and SA during 12 min sand impact test; (**f**) SEM image of the coating after sand impact test. In (**c**,**e**), WCA is the abbreviation of Water Contact Angle and SA is the abbreviation of Slip Angle, respectively.

3.4. Chemical Stability

When superhydrophobic coating is put into application, not only the influence of mechanical action on functional coating is desired to consider, but also the effect of chemical corrosive medium on coating under extreme conditions shall be estimated. To characterize the chemical resistance of the superhydrophobic coating, three kinds of solution were prepared. Strong acid solution (pH value of 2) was prepared using HCl, strong base solution (pH value of 12) was prepared using NaOH and salt solution with a concentration of 3.5% NaCl was prepared. The coated sample was soaked in each solution for 168 h and taken out every 8 h, washed with deionized water and dried. WCA and SA values were recorded after they were dried completely. The immersed sequence was strong acid solution, then strong base solution and salt solution last. The test results are shown in Figure 4a–c. The WCA value variations in strong acid, strong base and salt solution all manifested a slight decreasing trend. This small change was within the margin of error and the coating surface still maintained superhydrophobic characteristic. The SA variation of the coating in the three special solutions was small and the SA values still remained below 5°. The reason of the slight increase for SA is the enhanced electrostatic interaction at high ionic strength [32]. The holes among hierarchical structures might capture a large amount of air resulting in a reduction of direct contact area between corrosive liquid and coating. Thus, the surface of coating C5 could still preserve its superhydrophobic property.

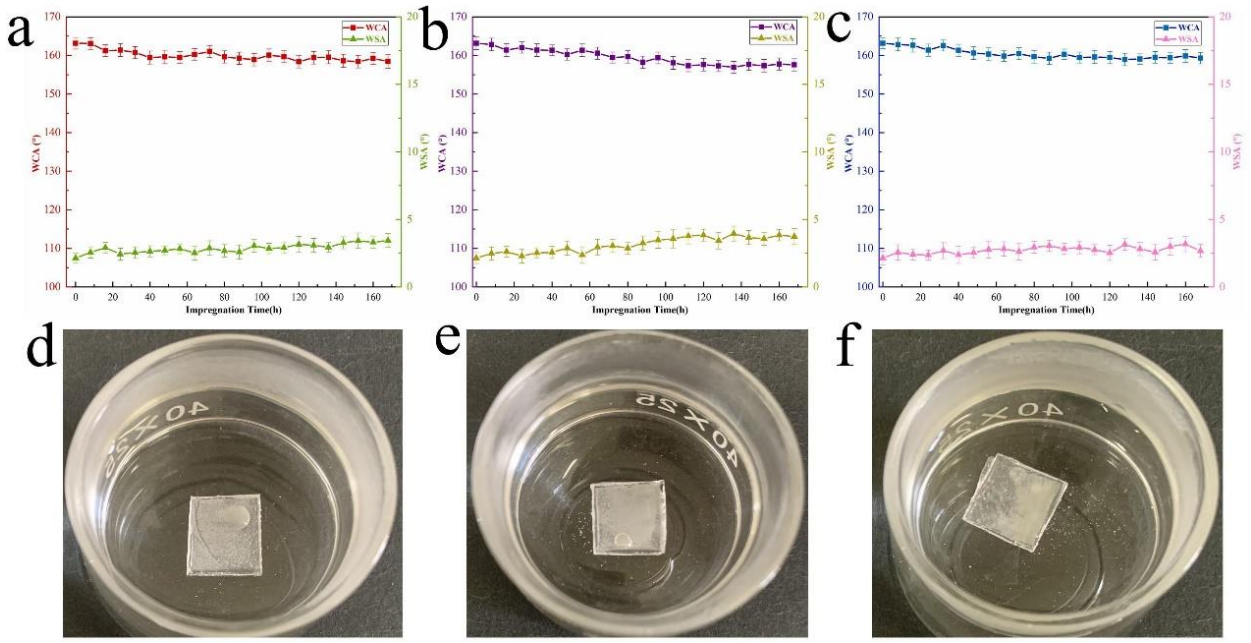

Figure 4. (**a**) WCA and SA variation trend of coating C5 immersed in HCl solution; (**b**) WCA and SA variation trend of coating C5 immersed in NaOH solution; (**c**) WCA and SA variation trend of coating C5 immersed in NaCl solution; (**d**) photograph of sample immersion state in HCl solution; (**e**) photograph of sample immersion state in NaOH solution; (**f**) photograph of sample immersion state in NaCl solution. In (**a**–**c**), WCA is the abbreviation of Water Contact Angle and SA is the abbreviation of Slip Angle, respectively.

4. Conclusions

In summary, transparent superhydrophobic coating with good mechanical and chemical stability was developed by UV curable method. Attributed to POSS component as well as hierarchical structures induced, the coating is prone to be superhydrophobic. With the increased amount of POSS component, hydrophobicity is improved while the transmittance is decreased. To balance super-hydrophobicity and transmittance, the coating prepared from 65% POSS component is considered as the optimal choice. The water contact angle of this coating is greater than 150° and the sliding angle from this coating is less than 10°, implying its super-hydrophobicity. The coating cured from the 65% POSS component displays preferable transmittance about 76.8%. Compared to the UV-cured commercial coatings, the coating adhesion is enhanced at least two levels. Water contact angle decreased a little after undergoing water droplet impact. Since part of hierarchical morphology was damaged after sand particle impact, super-hydrophobicity turned to hydrophobicity although the water contact angle was very close to 150°. Super-hydrophobicity was preserved after immersion in HCl solution (pH = 2), NaOH solution (pH = 12) and 3.5% NaCl solution, implying chemical resistance. This UV-curable coating containing a POSS component is possible for applying in outdoor transparent optical products. Moreover, the fabrication method is simple and has applied in many industry fields for large-scale production. Large-scale production of the transparent superhydrophobic coating has potential.

Author Contributions: Conceptualization and methodology, W.Z. and J.H.; analysis and resources, W.Z. and Y.X.; writing—original draft preparation, W.Z.; writing—review and editing, X.D. and J.H. All authors have read and agreed to the published version of the manuscript.

Funding: This research received no external funding.

Institutional Review Board Statement: Not applicable.

Informed Consent Statement: Not applicable.

Data Availability Statement: Not applicable.

Conflicts of Interest: The authors declare no conflict of interest.

References

1. Neinhuis, C.; Barthlott, W. Characterization and distribution of water-repellent, self-cleaning plant surfaces. *Ann. Bot.* **1997**, *79*, 667–677. [CrossRef]
2. Gao, L.C.; McCarthy, T.J. The "lotus effect" explained: Two reasons why two length scales of topography are important. *Langmuir* **2006**, *22*, 2966–2967. [CrossRef]
3. Gao, X.F.; Jiang, L. Water-repellent legs of water striders. *Nature* **2004**, *432*, 36. [CrossRef] [PubMed]
4. Lum, K.; Chandler, D.; Weeks, J.D. Hydrophobicity at small and large length scales. *J. Phys. Chem. B* **1999**, *103*, 4570–4577. [CrossRef]
5. Chen, J.; Yuan, L.; Shi, C.; Wu, C.; Long, Z.; Qiao, H.; Wang, K.; Fan, Q.H. Nature-Inspired Hierarchical Protrusion Structure Construction for Washable and Wear-Resistant Superhydrophobic Textiles with Self-Cleaning Ability. *ACS Appl. Mater. Interfaces* **2021**, *13*, 18142–18151. [CrossRef] [PubMed]
6. Jin, H.; Tian, L.; Bing, W.; Zhao, J.; Ren, L. Bioinspired marine antifouling coatings: Status, prospects, and future. *Prog. Mater. Sci.* **2022**, *124*, 100889. [CrossRef]
7. Liu, Y.; Fu, K.; Liu, J.; Tian, Y.; Zhang, H.; Wang, R.; Zhang, B.; Zhang, H.; Zhou, F.; Zhang, Q. Design and preparation of a multi-fluorination organic superhydrophobic coating with high mechanical robustness and icing delay ability. *Appl. Surf. Sci.* **2019**, *497*, 143663. [CrossRef]
8. Jia, L.; Sun, J.; Li, X.; Zhang, X.; Chen, L.; Tian, X. Preparation and Anti-frost Performance of PDMS-SiO_2/SS Superhydrophobic Coating. *Coatings* **2020**, *10*, 1051. [CrossRef]
9. Nie, Y.; Ma, S.; Tian, M.; Zhang, Q.; Huang, J.; Cao, M.; Li, Y.; Sun, L.; Pan, J.; Wang, Y.; et al. Superhydrophobic silane-based surface coatings on metal surface with nanoparticles hybridization to enhance anticorrosion efficiency, wearing resistance and antimicrobial ability. *Surf. Coat. Technol.* **2021**, *410*, 126966. [CrossRef]
10. Zhang, J.; Zhang, L.; Gong, X. Design and fabrication of polydopamine based superhydrophobic fabrics for efficient oil-water separation. *Soft Matter* **2021**, *17*, 6542–6551. [CrossRef] [PubMed]
11. Shao, J.; Sheng, W.; Wang, C.; Ye, Y. Solvent-free fabrication of tough self-crosslinkable short-fluorinated copolymer nanocoatings for ultradurable superhydrophobic fabrics. *Chem. Eng. J.* **2021**, *416*, 128043. [CrossRef]
12. Jang, G.G.; Smith, D.B.; List, F.A.; Lee, D.F.; Ievlev, A.V.; Collins, L.; Park, J.; Polizos, G. The anti-soiling performance of highly reflective superhydrophobic nanoparticle-textured mirrors. *Nanoscale* **2018**, *10*, 14600–14612. [CrossRef] [PubMed]
13. Lee, S.G.; Ham, D.S.; Lee, D.Y.; Bong, H.; Che, K. Transparent Superhydrophobic/Translucent Superamphiphobic Coatings Based on Silica-Fluoropolymer Hybrid Nanoparticles. *Langmuir* **2013**, *29*, 15051–15057. [CrossRef] [PubMed]
14. Sutha, S.; Suresh, S.; Raj, B.; Ravi, K.R. Transparent alumina based superhydrophobic self-cleaning coatings for solar cell cover glass applications. *Sol. Energy Mater. Sol. Cells* **2017**, *165*, 128–137. [CrossRef]
15. Torun, I.; Celik, N.; Hancer, M.; Es, F.; Emir, C.; Turan, R.; Onses, M.S. Water Impact Resistant and Antireflective Superhydrophobic Surfaces Fabricated by Spray Coating of Nanoparticles: Interface Engineering via End-Grafted Polymers. *Macromolecules* **2018**, *51*, 10011–10020. [CrossRef]
16. Xi, Y.; Yang, Z.; Zhang, J. Fabrication of superhydrophobic bilayer composite coating for roof cooling and cleaning. *Constr. Build. Mater.* **2021**, *291*, 123283. [CrossRef]
17. Zhan, W.; Wang, W.; Xiao, Z.; Yu, X.; Zhang, Y. Water-free dedusting on antireflective glass with durable superhydrophobicity. *Surf. Coat. Technol.* **2018**, *356*, 123–131. [CrossRef]
18. Allione, M.; Limongi, T.; Marini, M.; Torre, B.; Zhang, P.; Moretti, M.; Perozziello, G.; Candeloro, P.; Napione, L.; Pirri, C.F.; et al. Micro/Nanopatterned Superhydrophobic Surfaces Fabrication for Biomolecules and Biomaterials Manipulation and Analysis. *Micromachines* **2021**, *12*, 1501. [CrossRef]
19. Wang, J.; Chen, H. Fabrication of a superhydrophobic surface by a template-assisted chemical deposition method. *Mater. Express* **2020**, *10*, 1346–1351. [CrossRef]
20. Wei, D.; Wang, J.; Liu, Y.; Wang, D.; Li, S.; Wang, H. Controllable superhydrophobic surfaces with tunable adhesion on Mg alloys by a simple etching method and its corrosion inhibition performance. *Chem. Eng. J.* **2021**, *404*, 126444. [CrossRef]
21. Chen, F.; Xiang, W.; Yin, S.; Huang, S. Magnetically Responsive Superhydrophobic Surface with Switchable Adhesivity Based on Electrostatic Air Spray Deposition. *ACS Appl. Mater. Interfaces* **2021**, *13*, 20885–20896. [CrossRef]
22. Pratiwi, N.; Zulhadjri; Arief, S.; Admi; Wellia, D.V. Self-cleaning material based on superhydrophobic coatings through an environmentally friendly sol-gel method. *J. Sol-Gel Sci. Technol.* **2020**, *96*, 669–678. [CrossRef]
23. Zhang, L.; Sun, L.; Zhang, Z.; Wang, Y.; Yang, Z.; Liu, C.; Li, Z.; Zhao, Y. Bioinspired superhydrophobic surface by hierarchically colloidal assembling of microparticles and colloidal nanoparticles. *Chem. Eng. J.* **2020**, *394*, 125008. [CrossRef]
24. Biria, S.; Hosein, I.D. Superhydrophobic Microporous Substrates via Photocuring: Coupling Optical Pattern Formation to Phase Separation for Process Tunable Pore Architectures. *ACS Appl. Mater. Interfaces* **2018**, *10*, 3094–3105. [CrossRef]
25. Jiang, S.; Meng, X.; Chen, B.; Wang, N.; Chen, G. Electrospinning superhydrophobic-superoleophilic PVDF-SiO_2 nanofibers membrane for oil-water separation. *J. Appl. Polym. Sci.* **2020**, *137*, 49546. [CrossRef]

26. Zeng, Q.; Zhou, H.; Huang, J.; Guo, Z. Review on the recent development of durable superhydrophobic materials for practical applications. *Nanoscale* **2021**, *13*, 11734–11764. [CrossRef]
27. Zhou, H.; Ye, Q.; Xu, J. Polyhedral oligomeric silsesquioxane-based hybrid materials and their applications. *Mater. Chem. Front.* **2017**, *1*, 212–230. [CrossRef]
28. Chrusciel, J.J.; Lesniak, E. Modification of epoxy resins with functional silanes, polysiloxanes, silsesquioxanes, silica and silicates. *Prog. Polym. Sci.* **2015**, *41*, 67–121. [CrossRef]
29. Wang, L.; Zhang, C.; Zheng, S. Organic-inorganic poly(hydroxyether of bisphenol A) copolymers with double-decker silsesquioxane in the main chains. *J. Mater. Chem.* **2011**, *21*, 19344–19352. [CrossRef]
30. Zhang, X.; Ma, W.; Zhang, S.; Huang, H.; Ouyang, L.; Peng, W.; Ye, J.; Chen, C. A Comparative Study of Adhesion Evaluation Methods on Ophthalmic AR Coating Lens. *Coatings* **2020**, *10*, 979. [CrossRef]
31. Zhang, P.; Qin, B.; Xia, J. UV Curable Robust Durable Hydrophobic Coating Based on Epoxy Polyhedral Oligomeric Silsesquioxanes (EP-POSS) and Their Derivatives. *ACS Omega* **2022**, *7*, 17108–17118. [CrossRef] [PubMed]
32. Xu, C.L.; Song, F.; Wang, X.L.; Wang, Y.Z. Surface modification with hierarchical CuO arrays toward a flexible, durable superhydrophobic and self-cleaning material. *Chem. Eng. J.* **2017**, *313*, 1328–1334. [CrossRef]